Negative-index metamaterial at 780 nm wavelength

G. Dolling and M. Wegener

Institut für Angewandte Physik and DFG-Center for Functional Nanostructures (CFN), Universität Karlsruhe (TH), D-76131 Karlsruhe, Germany

C. M. Soukoulis

Ames Laboratory and Department of Physics and Astronomy, Iowa State University, Ames, Iowa 50011, USA

S. Linden

Institut für Nanotechnologie, Forschungszentrum Karlsruhe in der Helmholtz-Gemeinschaft, D-76021 Karlsruhe, Germany

Received August 23, 2006; revised September 28, 2006; accepted October 2, 2006; posted October 5, 2006 (Doc. ID 74376); published December 13, 2006

We further miniaturize a recently established silver-based negative-index metamaterial design. By comparing transmittance, reflectance, and phase-sensitive time-of-flight experiments with theory, we infer a real part of the refractive index of −0.6 at a 780 nm wavelength—which is visible in the laboratory. © 2006 Optical Society of America

OCIS codes: 160.4760, 260.5740.

Photonic metamaterials are tailored artificial optical materials composed of subwavelength metallic building blocks that can be viewed as nanoscale electronic circuits. These building blocks or "photonic atoms" are densely packed into an effective material such that the operation wavelength λ is ideally much larger than the lattice constant a. Along these lines, highly unusual material properties become accessible, e.g., a negative index of refraction,[1,2] which has recently reached operation wavelengths of 2,[3] 1.5,[4] 1.5,[5] and 1.4 μm.[6] In this Letter we demonstrate a negative index of refraction at the red end of the visible spectrum (780 nm wavelength) for what is the first time to our knowledge.

The physics of the particular sample or circuit design[7] used and miniaturized here has been described previously in work at lower frequencies.[3,5,6] In brief, for the polarization configuration shown in Fig. 1(a), the metamaterial can be viewed as composed of two sets of subcircuits or "atoms": (i) a coil with inductance L in series with two capacitors with net capacitance C as an LC circuit, providing a magnetic resonance at the LC resonance frequency,[8] and (ii) long metallic wires, acting like a diluted metal below the effective plasma frequency of the arrangement.[9] The negative magnetic permeability from (i) and the negative electric permittivity from (ii) lead to a negative index of refraction.[1,2] We use silver as a constituent material because silver is known to introduce significantly lower losses[10] than, e.g., gold at visible frequencies. The choice of the dielectric spacer material is uncritical; we use MgF_2. In numerical calculations, the design parameters have carefully been optimized for optical performance. Results from the best fabricated sample are shown here.

Fabrication employs standard electron-beam lithography, electron-beam evaporation of the constituent materials, and a liftoff procedure. All samples are located on glass substrate, coated with a 5 nm thin film of indium tin oxide (ITO) to avoid charging effects in the electron-beam-writing process (the ITO layer is irrelevant for the optical performance). The electron micrograph of the best sample (100 μm $\times$ 100 μm footprint) shown in Fig. 1(c) reveals good large-scale homogeneity as well as a 68 nm minimum lateral feature size at 97 nm thickness of the $Ag-MgF_2-Ag$ sandwich. This aspect ratio (i.e., height/width), exceeding unity, poses significant fabrication challenges. Compared with our previous choice of parameters at lower frequencies,[5,6] especially the relative thickness of the metal wires oriented along the electric field vector [i.e., the ratio w_y/a_y in Fig. 1(b)] had to be increased. This step increases the effective plasma frequency, which needs to be above the operation frequency to yield a negative electric permittivity. The increased aspect ratio leads to a sidewall roughness of the order of 10 nm [see inset of Fig. 1(c)].

Figure 2(a) shows measured normal-incidence intensity transmittance and reflectance spectra (taken with a 5° half-opening angle) of this metamaterial sample. The bare glass substrate and a silver mirror serve as references. Shown in Fig. 2(b) is the corresponding theoretical result based on numerical three-dimensional finite-difference time-domain calculations performed by using the commercial software package CST Micro Wave Studio. The geometrical parameters have already been indicated in Fig. 1(b); optical material parameters taken are the MgF_2 refractive index $n_{MgF_2}=1.38$, glass substrate index $n_{substrate}=1.5$, and the Drude model for silver with plasma frequency $\omega_{pl}=1.37\times10^{16}\ s^{-1}$ and damping or collision frequency $\omega_{col}=9\times10^{13}\ s^{-1}$. At the frequencies of interest here the Drude model is an adequate description of the actual silver dielectric function.[10] The quoted damping has been chosen to match the experiment in the present work and especially comprises broadening effects due to any type of sample imperfection (e.g., granularity of the metal film or inhomogeneous broadening). The chosen damping is three times larger than the literature value.[10] It is

0146-9592/07/010053-3/$15.00

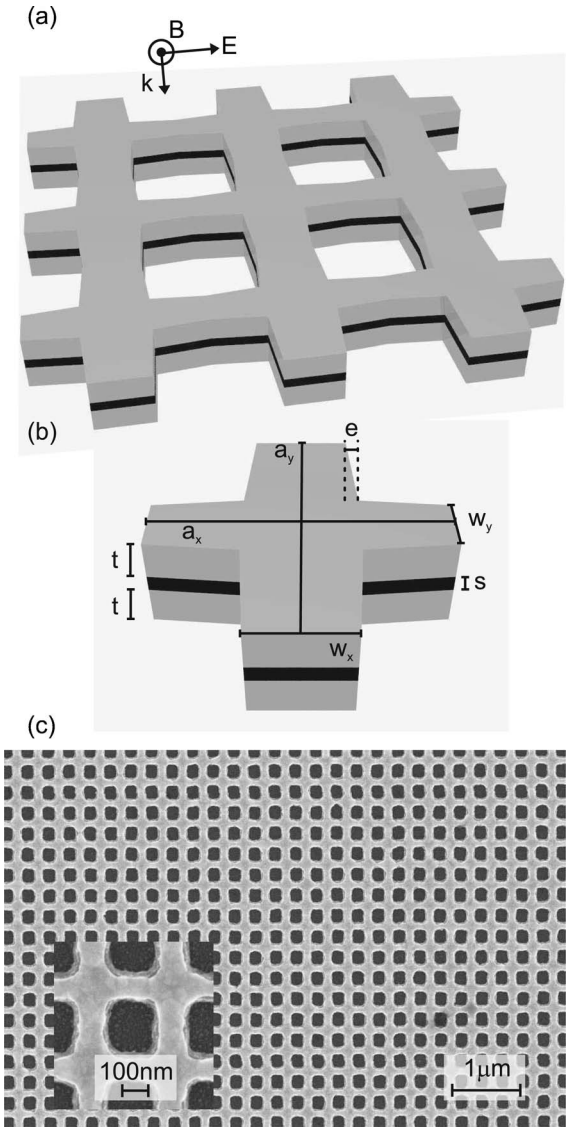

Fig. 1. (a) Scheme of the metamaterial and polarization configuration. (b) Unit cell of the structure with definition of parameters: lattice constant $a_x = a_y = 300$ nm, $w_x = 102$ nm, $w_y = 68$ nm, $t = 40$ nm, $s = 17$ nm, and $e_x = e_y = e = 8$ nm. The last parameter describes small deviations from rectangular shape. (c) Top-view electron micrograph of the sample employed in Figs. 2 and 3. Inset, magnified view.

important that the exact same set of parameters will also be used below for the theoretical analysis of the interferometric experiments as well as for effective-parameter retrieval.

An unambiguous determination of effective material parameters, especially of the phase velocity $c = c_0/n$, additionally requires phase-sensitive experiments. The details and the errors of the phase-sensitive time-of-flight experiment based on a compact and passively stable Michelson interferometer were described previously by us,[5] albeit in a different wavelength regime. In essence, we record two interferograms, one with the metamaterial sample on its glass substrate in one of the interferometer arms, and a second interferogram with just the glass substrate by laterally moving the metamaterial out of the optical path. All mechanical motions are computer controlled and realized by precise and calibrated piezoelectric actuators. The corresponding shift on the interferometer time delay axis yields the phase delay due to the metamaterial. By tuning the center wavelength of the incident Gaussian transform-limited 125 fs pulses, derived from a commercial mode-locked Ti:sapphire laser (Spectra-Physics Tsunami), and by repeating the described procedure for each wavelength, we measure phase-delay spectra. Simultaneously and similarly, we infer the shift between the two Gaussian interferogram envelopes at each wavelength, which provides us with the group-delay spectra. In essence, the group-delay spectrum is the spectral derivative of the phase-delay spectrum. Thus the group-delay spectrum sensitively depends on the damping. Corresponding data (dots) are shown in Figs. 3(a) and 3(b) together with numerical calculations (solid curves), in which we derive the interferograms from the complex sample electric field transmittance for the femtosecond pulse parameters as in the experiment and then proceed with the analysis as in the experiment. Clearly, all effects due to the finite spectral width of the pulses are appropriately accounted for in this manner. Finally, we retrieve[11] the effective material parameters from theory and depict them in Fig. 3(c). These retrieved parameters refer to a fictitious homogeneous film on the glass substrate with a thickness identical to that of the metamaterial ($d = 97$ nm) and complex transmittance and reflectance properties strictly identical to those of the metamaterial on the glass substrate. From the increasing relative importance of the imaginary part of the silver dielectric function for frequencies (even remotely) approaching the plasma frequency, one expects increased losses.

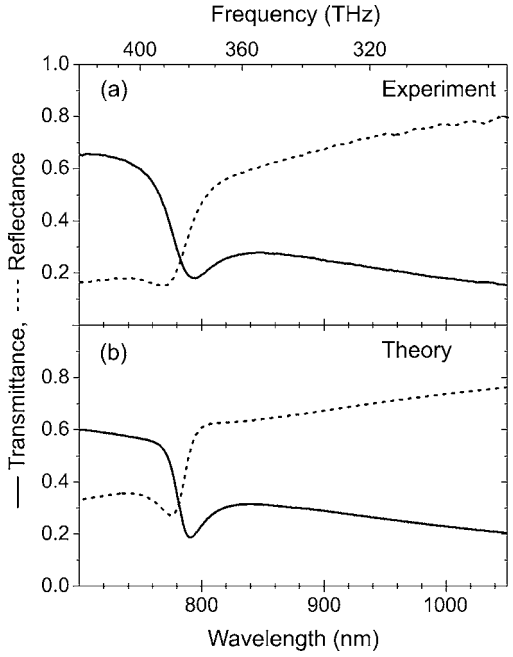

Fig. 2. (a) Measured transmittance (solid) and reflectance (dashed) spectrum of the negative-index metamaterial described in Fig. 1 for the polarization configuration of Fig. 1(a). (b) Corresponding theoretical calculation. The same parameters are used in the calculations depicted in Fig. 3.

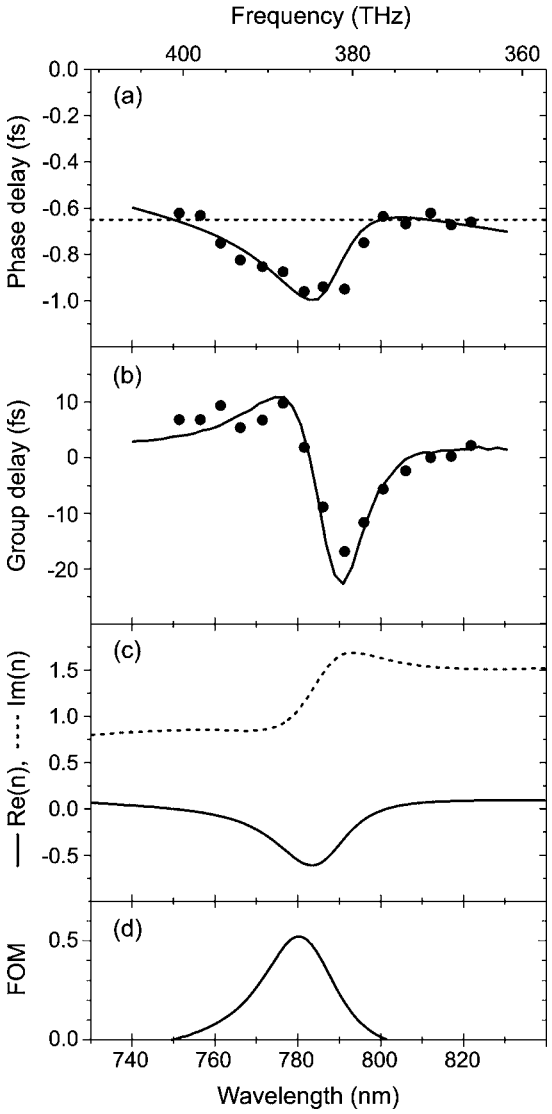

Fig. 3. (a) Measured (dots) phase delay versus laser center wavelength for a pulse propagating through the metamaterial sample characterized in Figs. 1 and 2 and for the polarization configuration depicted in Fig. 1(a). The solid curve is the corresponding theoretical calculation. The dashed horizontal line corresponds to $\mathrm{Re}(n)=0$.[5] (b) Group delay versus wavelength. (c) Retrieved real (solid) and imaginary (dashed) part of the effective refractive index n. (d) Resulting figure of merit $\mathrm{FOM}=-\mathrm{Re}(n)/\mathrm{Im}(n)$. The same set of sample parameters is used in all calculations shown in Figs. 2 and 3.

Indeed, the figure of merit (FOM) shown in Fig. 3(d) and defined via $\mathrm{FOM}=-\mathrm{Re}(n)/\mathrm{Im}(n)$, is FOM=0.5 at best, while best values of FOM=3 have recently been achieved at 1.4 μm wavelength by us.[6] Still, the obtained value of FOM=0.5 is comparable with previous work at longer wavelengths.[3–5] Possibly the FOM can be increased by stacking several layers.[12]

Obviously, the experimental results agree well with theory, which consistently describes transmittance (solid curves in Fig. 2), reflectance (dashed curves in Fig. 2), and phase-delay [Fig. 3(a)], as well as group-delay spectra [Fig. 3(b)], all with one set of parameters. Thus the effective material parameters, especially the negative real part of n [Fig. 3(c)], retrieved from the same theory and the same parameters can be considered as very trustworthy. A determination on the basis of, e.g., intensity reflectance spectra alone would be ambiguous and not at all reliable based on our experience.

In conclusion, we have demonstrated a metamaterial with an effective real part of the index of refraction of −0.6 around 780 nm wavelength. This wavelength can easily be seen with the naked eye in our laser experiments. Our work goes beyond previous work in the visible,[13] which claimed a negative magnetic permeability. Phase-sensitive time-of-flight experiments give direct experimental evidence for the negative phase velocity of light. Studying the group velocity in parallel provides a sensitive consistency check of our analysis.

We acknowledge support by the Deutsche Forschungsgemeinschaft (DFG) and the State of Baden-Württemberg through the DFG-Center for Functional Nanostructures (CFN) within subproject A1.5. The research of S. Linden is further supported through a Helmholtz-Hochschul-Nachwuchsgruppe (VH-NG-232), that of C. M. Soukoulis by the Alexander von Humboldt senior scientist award 2002, by Ames Laboratory (contract W-7405-Eng-82), and EU projects PHOREMOST and METAMORPHOSE, and DARPA (HR0011-05-C-0068). C. M. Soukoulis is also with the Institute of Electronic Structure and Laser at FORTH and the Department of Materials Science and Technology, University of Crete, Heraklion, Crete, Greece. G. Dolling's e-mail address is gunnar.dolling@physik.uni-karlsruhe.de.

References

1. R. A. Shelby, D. R. Smith, and S. Schultz, Science **292**, 77 (2001).
2. D. R. Smith, J. B. Pendry, and M. C. K. Wiltshire, Science **305**, 788 (2004).
3. S. Zhang, W. Fan, N. C. Panoiu, K. J. Malloy, R. M. Osgood, and S. R. J. Brueck, Phys. Rev. Lett. **95**, 137404 (2005).
4. V. M. Shalaev, W. Cai, U. K. Chettiar, H. Yuan, A. K. Sarychev, V. P. Drachev, and A. V. Kildishev, Opt. Lett. **30**, 3356 (2005).
5. G. Dolling, C. Enkrich, M. Wegener, C. M. Soukoulis, and S. Linden, Science **312**, 892 (2006).
6. G. Dolling, C. Enkrich, M. Wegener, C. M. Soukoulis, and S. Linden, Opt. Lett. **31**, 1800 (2006).
7. S. Zhang, W. Fan, K. J. Malloy, S. R. J. Brueck, N. C. Panoiu, and R. M. Osgood, Opt. Express **13**, 4922 (2005).
8. J. B. Pendry, A. J. Holden, D. J. Robbins, and W. J. Stewart, IEEE Trans. Microwave Theory Tech. **47**, 2075 (1999).
9. J. B. Pendry, A. J. Holden, W. J. Stewart, and I. Youngs, Phys. Rev. Lett. **76**, 4773 (1996).
10. P. B. Johnson and R. W. Christy, Phys. Rev. B **6**, 4370 (1972).
11. D. R. Smith, S. Schultz, P. Marko, and C. M. Soukoulis, Phys. Rev. B **65**, 195104 (2002).
12. S. Zhang, W. Fan, N. C. Panoiu, K. J. Malloy, R. M. Osgood, and S. R. J. Brueck, Opt. Express **14**, 6778 (2006).
13. A. N. Grigorenko, A. K. Geim, H. F. Gleeson, Y. Zhang, A. A. Firsov, I. Y. Khrushchev, and J. Petrovic, Nature **438**, 335 (2005).